

---

# Value of information of in-situ inspections of mooring lines

Journal of Risk and Reliability  
XX(X):1–13  
©The Author(s) 2020  
Reprints and permission:  
sagepub.co.uk/journalsPermissions.nav  
DOI: 10.1177/ToBeAssigned  
www.sagepub.com/

SAGE

Jorge Mendoza<sup>1</sup>, Jacopo Paglia<sup>1</sup>, Jo Eidsvik<sup>1</sup> and Jochen Köhler<sup>1</sup>

## Abstract

Mooring systems that are used to secure position keeping of floating offshore oil and gas facilities are subject to deterioration processes, such as pitting corrosion and fatigue crack growth. Past investigations show that pitting corrosion has a significant effect on reducing the fatigue resistance of mooring chain links. In-situ inspections are essential to monitor the development of the corrosion condition of the components of mooring systems and ensure sufficient structural safety. Unfortunately, offshore inspection campaigns require large financial commitments. As a consequence, inspecting all structural components is unfeasible. This article proposes to use value of information analysis to rank identified inspection alternatives. A Bayesian Network is proposed to model the statistical dependence of the corrosion deterioration among chain links at different locations of the mooring system. This is used to efficiently update the estimation of the corrosion condition of the complete mooring system given evidence from local observations and to reassess the structural reliability of the system. A case study is presented to illustrate the application of the framework.

## Keywords

Bayesian network, Value of information, Pitting corrosion, Fatigue, Mooring line, Structural system

## Introduction

Mooring systems secure the position keeping of floating offshore platforms and consist of several mooring lines that connect the platform to an anchor on the seabed. The main structural part of mooring lines is usually constituted by steel chains, although alternative configurations and materials exist, such as synthetic fiber rope, steel wire rope or a combination of all of them.<sup>1</sup> In this article, we focus on mooring lines constituted by studless steel chains. The integrity of mooring chains can be treated as a serial system, since failure of a single link leads to structural failure of the complete mooring line. A mooring line failure increases the load level on the adjacent lines and thereby increases the probability of progressive collapse of the mooring system. This is associated with large environmental and economical consequences, such as oil spill, loss of production and loss of reputation of the involved companies. Consequently, the detection of failures in a mooring line system is usually followed by operation shutdown, which is associated with large economical loss. Manufacturing of chain links is costly and it demands large amounts of steel. Furthermore, integrity management measures of mooring systems require large financial investments, making it unfeasible to inspect

all components or to apply mitigation measures when any deterioration is observed. Therefore, resources invested in risk mitigation need to be carefully allocated to ensure a cost-efficient and safe operation.

Mooring lines are subject to large environmental cyclic loading while being exposed to a highly corrosive environment, leading to fatigue and corrosion deterioration. Fontaine et al.<sup>1</sup> report that these deterioration processes account for the majority of observed mooring line failures. Recommended practice guidelines, such as API RP 2SK<sup>2</sup>, and industry standards, such as ISO 19901-7:2013<sup>3</sup> and DNVGL-OS-E301<sup>4</sup>, consider that these deterioration processes can be addressed independently from each other for the design and integrity management of mooring lines. Corrosion deterioration is typically assessed by estimating the lifetime chain diameter reduction, assuming uniform corrosion and wear per year. Fatigue design is commonly conducted using S-N curves, which are curves that assess the

---

<sup>1</sup>Norwegian University of Science and Technology

### Corresponding author:

Jorge Mendoza, NTNU, Høgskoleringen 1, 7491 Trondheim, Norway.

Email: jorge.m.espinosa@ntnu.no

number of cycles to fatigue failure for a given cyclic stress range.

Several investigations emphasize the significant effect of corrosion on the fatigue life of mooring chains.<sup>5-7</sup> Structural failure is in general not a linear superposition of the effects of corrosion and fatigue, but a complex combination of phenomena. Among the several ways in which the two deterioration phenomena interact, it is identified that localized corrosion, commonly known as corrosion pits, act as stress raisers on the chain link surface, fostering fatigue crack initiation.<sup>8,9</sup> Gabrielsen et al.<sup>10</sup> report results of visual surface inspection of retrieved mooring chains, which reveal significant local wear at the contact region of links close to the winch on the installations and severe spatially distributed pitting corrosion. Fatigue testing in laboratory conditions of these retrieved links suggests that surface roughness and pitting depth are the main indicators of the reduction of fatigue resistance, which is aligned with other research studies.<sup>11</sup> The unaccounted interaction between these phenomena in design standards may explain why observed failure rates of mooring lines are larger than expected and admissible.<sup>1,12</sup>

The deterioration conditions of the different chain links constituting the mooring system are statistically dependent. Dependence among different locations is mainly due to common influencing factors related to the environment and to the manufacturing process of the links. Examples of such factors are material parameters, load history, pH, temperature and the amount of dissolved oxygen. It is important to take this dependence into account because (i) it affects the structural reliability of the system<sup>13</sup> and consequently, integrity management decisions; (ii) it has a large impact on the amount of information to be learned from local inspections at discrete points in time, since information gathered at one location can be used to update the belief on the deterioration condition at other parts of the structural system.<sup>14</sup> Hence, the statistical modeling affects optimal planning of inspection campaigns.

This study pursues to inform and support integrity management decisions regarding the allocation of discrete inspections in mooring line systems. For that purpose, we propose a Bayesian Network (BN) to model the dependence in the surface condition within the components of the mooring system and its effect on the fatigue life of the mooring lines and the structural integrity of the mooring system. Value of information (VOI) analysis is then used to assess the most valuable data to collect.<sup>15,16</sup> The use of BNs for modeling the problem helps with the integration of observations (evidence) about variables of interest and

to efficiently perform statistical inference. BNs have been used for decision making support and VOI analysis in various contexts.<sup>17,18</sup> Arzaghi et al.<sup>19</sup> use a dynamical BN to study pitting corrosion and fatigue degradation over time for submerged pipelines. Li et al.<sup>20</sup> apply BNs for modeling corrosion of pipelines and to study an optimal maintenance plan with a particular focus on risk-based maintenance. Rather than providing a maintenance plan, the present study focuses on using VOI analysis to assess the most valuable data to gather in order to inform integrity management decisions for mooring systems.

## Problem setting

The structural integrity of the mooring system of a floating oil and gas production unit is regarded. The decision maker is the operator of the production unit. At a given point in time of the service life of the mooring system, the decision maker is to efficiently plan an inspection campaign. An inspection campaign provides information on the corrosion condition of one or several chain segments. Possible decisions that the decision maker can choose from are to inspect any given number of segments, or not to conduct any inspection. The gathered evidence is used to inform actions on the structural system, such as to repair or replace any line segment, or to do nothing. It is assumed that both replacement and repair of segments set their corrosion condition back to completely uncorroded.

The structural system is subdivided into four hierarchical levels, as illustrated in Figure 1. The first level corresponds to the complete system of mooring chains, which is constituted by a set of  $M \in \mathbb{N}$  clusters of mooring lines  $\mathcal{C} = \{C_1, \dots, C_M\}$ . At the second level, a cluster  $C_j$  is comprised of  $N_j \in \mathbb{N}$  mooring lines  $\mathcal{L}_j = \{L_{1,j}, \dots, L_{N_j,j}\}$ . The third level is the mooring line level, where line  $L_{i,j}$  is subdivided into  $p \in \mathbb{N}$  mooring line segments  $\mathcal{S}_{i,j} = \{S_{i,j,1}, \dots, S_{i,j,p}\}$ , with each segment containing a number of chain links with approximately the same expected deterioration condition. Finally, the fourth level is constituted by the line segment.

Information about the corrosion condition of mooring links can be gathered using *in-situ* techniques, for instance by surface scanning using a remotely operated vehicle (ROV). The subdivision of a mooring line into segments should be performed so that one local observation, say of the surface of one link, can be used to characterize the condition of the entire segment with sufficient accuracy. By embedding the presented hierarchical structure in a probabilistic model, information retrieved from a particular segment can be used to update the belief on the corrosion condition of the entire

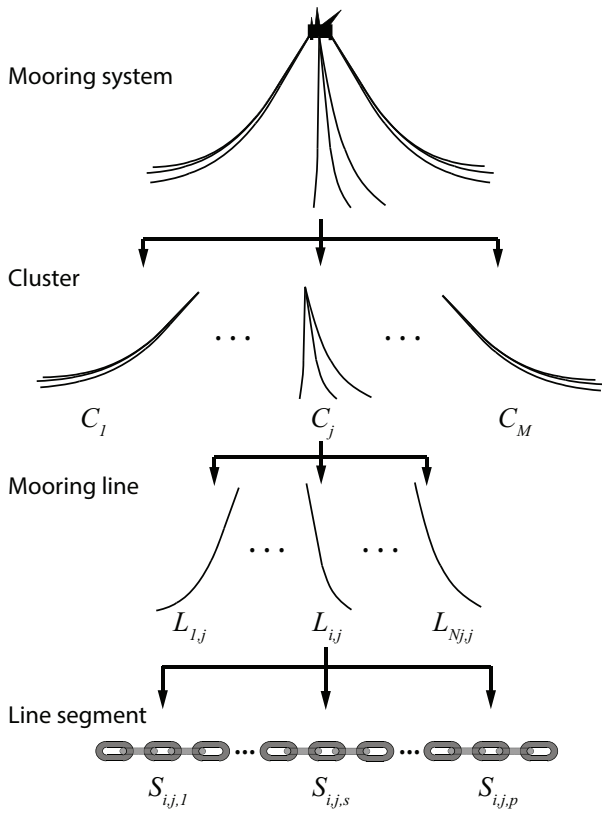


**Figure 1.** Hierarchical organization of the components of the mooring system.

mooring system. Prior knowledge is required to train the model for the corrosion conditions. This is done using state of the art physics-based models, as described below. Given a model that relates corrosion condition and fatigue resistance, the structural reliability of the mooring system can be subsequently reassessed when more information is available.

Decisions regarding which segment to inspect are ranked based on VOI analysis. The theoretical background of VOI analysis is briefly presented in the next section. An estimate of the structural reliability of the system is needed in order to conduct the VOI analysis. A BN is developed and used to relate the corrosion condition of the chain segments, including all available information at the decision point in time, with the structural reliability of the mooring system one year ahead. We use this estimate of the system reliability for the VOI analysis. This is a simplification, since inspection planning optimization is in general a sequential decision problem, i.e. inspection ranking at a given year depends on the subsequent inspection planning. Assessing the sequential decision problem is computationally demanding, since it would require to evaluate a dynamic BN in order to compute the evolution of the structural reliability in time and to explore a set of possible inspection alternatives which grows exponentially with the remaining service time of

the structure. Due to computational limitations, the authors approach this issue by treating it as a static problem in this article.

### Value of information of discrete inspections

Decisions on when and where inspections of the surface condition of mooring chain links are to be conducted are made with the intention to balance the large costs associated with these inspections and the value that they bring. Among the several approaches that one can regard to inform these decisions, VOI analysis is identified as a rational tool to make more conscious decisions by minimizing the expected costs. The value of conducting an inspection is a measure of the potential that retrieving new evidence has on triggering different actions upon the structural components of the system. At its roots, the VOI is the maximum monetary value that a decision maker should be willing to pay for a new observation.<sup>16</sup> In practice, the VOI associated with a variety of possible inspection schemes can be used to rank these schemes and to provide a useful basis for decision support.

Let  $a \in \mathcal{A}$  denote actions or alternatives that the decision maker can choose among. In the current application, these actions relate to repair, replace or do nothing for different combinations of segments, lines and clusters. The value function  $v(\mathbf{x}, a)$  describes the monetary value as a function of the alternative  $a$  and the uncertain variables of interest  $\mathbf{x}$ . Boldface notation is used to indicate that  $\mathbf{x}$  is a vector consisting of the indicators for the corrosion condition at the various segments, lines and clusters, and also the temperatures at different sea depths and other variables that contribute to a useful statistical representation of the system. Before any inspection is done, the decision maker will select the alternative that maximizes the expected value of  $v(\mathbf{x}, a)$ . This is called the prior value (PV), and it is defined as

$$PV = \max_{a \in \mathcal{A}} \{\mathbb{E}[v(\mathbf{x}, a)]\}. \quad (1)$$

Decisions on inspection planning are conducted prior to obtaining the information. The evaluation of inspection alternatives is based upon conditional values, given the observation outcomes. The preposterior value (PPV) integrates over all the possible observation outcomes

$$PPV_{\kappa} = \int \mathbf{y}_{\kappa} \max_{a \in \mathcal{A}} \{\mathbb{E}[v(\mathbf{x}, a) | \mathbf{y}_{\kappa}]\} \Pr(\mathbf{y}_{\kappa}) d\mathbf{y}_{\kappa}, \quad (2)$$

where the (possibly multivariate) retrieved data  $\mathbf{y}_{\kappa}$  denotes the outcome of inspection scheme  $\kappa$ . Note that there are many possible combinations of inspections schemes  $\kappa$ , such

as inspecting a given segment or a combination of them. One wants to choose these wisely so that inspection results  $\mathbf{y}_\kappa$  are likely to improve the actions related to repair or replacement.

The VOI associated with a potential inspection alternative  $\kappa$  is obtained by subtracting the PV to the PPV

$$\text{VOI}_\kappa = \text{PPV}_\kappa - \text{PV}. \quad (3)$$

Given the fact that inspections come with a cost, the decision maker can compare the VOI with the inspection cost ( $c_\kappa$ ), and acquire data only if  $\text{VOI}(\mathbf{y}_\kappa) - c_\kappa > 0$ . Moreover, one can rank inspection alternatives according to their information gain. The optimal inspection alternative is then

$$\kappa_{opt} = \arg \max_{\kappa} \text{PPV}_\kappa. \quad (4)$$

### Pit depth growth model

The division of the mooring line in smaller segments allows the modeling of statistical dependencies between segments of the same line at different depths and between segments of different lines. The physical variable of interest is the maximum pit depth  $d$ . When modeling  $d$ , it is necessary to consider the possible factors that can affect pit growth. Melchers<sup>21</sup> shows that the development of pitting in steel components immersed in seawater can be divided in two major phases: aerobic and anaerobic. Initially, during a period that can comprise some months to few years, pit depth growth is driven by anaerobic action and is, in general, significantly lower than the one caused by the subsequent phase. During this first phase, biological activity, water velocity and the amount of dissolved oxygen have relevant effects on the pit growth. For the remaining service life of the chain, the growth of corrosion pits is part of the anaerobic phase. Growth during this phase is largely caused by biological agents, such as sulfate-reducing bacteria (SRB). The water temperature is found to play a central role for the growth of SRB. Pits can reach extreme depths during this phase, which may lead to failure of the mooring line in combination with fatigue deterioration. Here, we focus on the second, anaerobic phase when modeling pit growth.

It is assumed, in accordance with the model by Melchers<sup>21</sup>, that the anaerobic phase starts right after the aerobic phase at a time  $t_a$ . This time is found to mainly depend on temperature  $T$  and its best estimate is represented by  $t_a^* = 6.61 \exp(-0.088T)$ . For a typical range of temperatures in the North Sea (between 6.9 to 19.0 °C),  $t_a^*$  varies between 3.6 and 1.2 years. At time  $t_a$ , the expected maximum pit depth, denoted  $\bar{d}$  is found as a function of

**Table 1.** Best estimates of the parameters of the maximum pit depth time propagation model.

Temperature	$f_{a_T}$	$t_a^*$ [years]	$a_T$	$b_T$
6.9°C	0.862	3.60	1.064	0.616
9.8°C	0.880	2.79	1.100	0.562
12.0°C	0.889	2.30	1.108	0.539
14.4°C	0.896	1.86	1.110	0.526
16.6°C	0.901	1.53	1.111	0.519
19.0°C	0.905	1.24	1.116	0.518

temperature

$$\bar{d}(t_a, T) = 0.99 \exp(-0.052T). \quad (5)$$

A piece-wise function is proposed by Melchers<sup>21</sup> to model the time evolution of the mean maximum pit depth, which is constituted by an initial non-linear growth curve followed by a linear one. At time  $t = t_a$ , the maximum pit depth grows fast with an initial slope  $r_{ap}$ , which depends on temperature  $T$  according to the following functional relationship

$$\left. \frac{\partial \bar{d}(t, T)}{\partial t} \right|_{t=t_a} = r_{ap} = 0.596 \exp(0.0526T). \quad (6)$$

Afterwards, the growth rate decreases until it reaches a constant value, which is modeled by a line with slope  $r_{sp}$  and intercept  $c_{sp}$ . In this study, the piece-wise function is simplified to a single power-law of the form

$$\bar{d}(t) = a_T \cdot (t - t_a^* f_{a_T})^{b_T} \quad t \geq t_a, \quad (7)$$

where the parameters  $a_T$  and  $b_T$  are estimated by applying the constraints in Eqs. (5) and (6) using a relaxation parameter  $f_{a_T}$ .

The model parameters are provided in Table 1 for a range of typical temperatures in the North Sea. Note that this simplified model is justified for short term predictions. For longer term predictions, say more than 15 years, the power

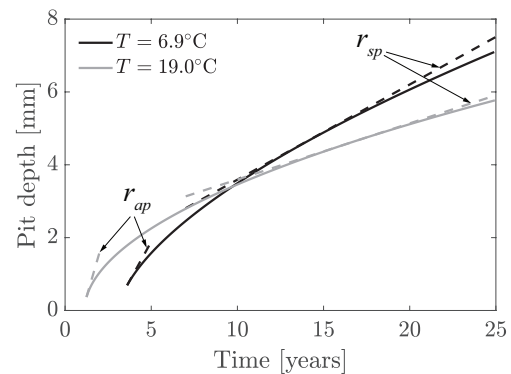


**Figure 2.** Time evolution model for the anaerobic phase of the expected maximum pit depth  $d$  for typical temperatures  $T$  in the North Sea.

low model may underestimate the growth in comparison with the piece-wise function, as shown in Figure 2. Nevertheless, such predictions are not needed for the purpose of inspection planning, since evidence is provided in shorter intervals. Figure 2 shows the time evolution model for the expected maximum pit for two temperatures.

The uncertainty associated with the prediction of the pit depth at a given time is taken into account with a multiplicative Log-normal error  $\delta_2$

$$d(t) = \delta_2 \bar{d}(t) \quad t \geq t_a, \quad (8)$$

where  $\bar{d}(t)$  is the expected maximum pit depth in Eq. (7) and  $\delta_2$  has mean value  $\mu_{\delta_2} = 1$  and standard deviation  $\sigma_{\delta_2}$ , which is varied to study its sensitivity later in the paper.

### Corrosion levels

It is assumed that the decision maker uses seven levels to characterize the corrosion condition, with  $\gamma_c = 1$  being the uncorroded state and  $\gamma_c = 7$  being associated with heavy corrosion and large pits. A corrosion level is assigned to a chain link by visual assessment conducted by trained personnel. The assignment synthesizes several aspects of the corrosion condition, such as the average cross-section reduction due to uniform corrosion, the number of pits and the distribution of pit depths and their shape. There is uncertainty associated with the assignment of corrosion levels due to the nature of the visual inspection. In the current case, the assignment of a corrosion level is assumed to be largely correlated with the maximum pit depth  $d$  present in the inspected specimen. This is consistent with the dependence among pit depths in a given chain link. The decision maker provides a probabilistic model of the distribution of the largest pit depth conditional on the corrosion level, see Table 2 and Figure 3.

In the BN, the corrosion levels are defined conditional on the maximum pit depths. Hence, for each segment, the probability of the corrosion level conditional on the

**Table 2.** Mean  $\mu$  and coefficient of variation (CoV) of the probability density function  $f_{D|\Gamma_c}(d|\gamma_c)$  of pit depth  $d$  conditional on the corrosion level.

Corrosion level	Distribution	$\mu$ [mm]	CoV [-]
1	Exponential	0.05	1.0
2	Normal	0.30	0.2
3	Normal	0.70	0.2
4	Normal	1.10	0.2
5	Normal	1.40	0.2
6	Normal	2.00	0.2
7	Normal	3.00	0.2

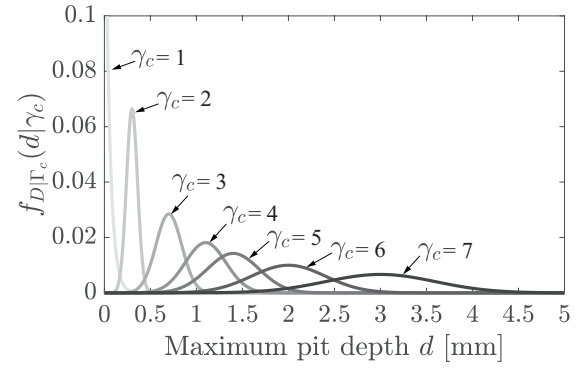


**Figure 3.** Probability density function  $f_{D|\Gamma_c}(d|\gamma_c)$  of pit depth  $d$  conditional on the corrosion level  $\Gamma_c = [1, 2, \dots, 7]$ .

maximum pit depth needs to be specified. This conditional probability is computed using the Bayes' formula

$$\Pr(\gamma_c|d) = \frac{\Pr(d|\gamma_c) \Pr(\gamma_c)}{\sum_{\gamma_c} \Pr(d|\gamma_c) \Pr(\gamma_c)}, \quad (9)$$

where  $f_{D|\Gamma_c}(d|\gamma_c)$  is the conditional probability density function of the maximum pit depth given the corrosion level and  $\Pr(\gamma_c)$  is the uniform distribution over the seven corrosion levels. In order to evaluate this equation, the continuous space of possible maximum pit depths ( $D \in \mathbb{R}^+$ ) is discretized.

### Effect of pitting corrosion on fatigue resistance

The following model is used to assess the combined effect of cyclic stresses and pitting corrosion on fatigue life

$$N_F(\Delta S, \gamma_c) = \delta_1 \cdot k \cdot \Delta S^{-m} \cdot \gamma_c^{\beta_2}, \quad (10)$$

where  $N_F$  is the number of cycles to failure,  $\Delta S$  are the fatigue stress ranges,  $\delta_1$  is the model uncertainty, and  $k$ ,  $m$  and  $\beta_2$  are regression parameters that mainly depend on the material characteristics and geometry of the structural component of interest. Here,  $\delta_1 = 10^\epsilon$ , with  $\epsilon$  being Normal distributed with zero mean and standard deviation  $\sigma_\epsilon$ . The model parameters are summarized in Table 3.

Fatigue damage is a cumulative process. As the result of a time dependent deterioration process, the probability

**Table 3.** Mean  $\mu$  and standard deviation  $\sigma$  of the parameters of the model in Eq. (10) for fatigue failure of a mooring line segment with studless chain links.

Parameter	Distribution	$\mu$	$\sigma$
$m$	Deterministic	3.0	0
$\log_{10} k$	Normal	11.200	0.100
$\beta_2$	Normal	-0.800	0.150
$\sigma_\epsilon$	Normal	0.170	0.030

of fatigue failure is typically represented by the cumulative probability of failure given a reference period  $T_{ref}$ . The accumulated fatigue damage at year  $t$  is denoted  $D(t)$ . For a given stress range  $\Delta S_i$  and corrosion level  $\gamma_c$ , a fatigue cycle  $i$  contributes to fatigue damage as

$$\Delta D_i(\Delta S_i, \gamma_c) = \frac{1}{N_F(\Delta S_i, \gamma_c)}. \quad (11)$$

Note that the stress range  $\Delta S_i$  is a realization of the process  $\Delta S(t)$ . The expected damage per cycle conditional on the corrosion level  $\mathbb{E}[D_i|\gamma_c]$  is used in the following to simplify the computation of the cumulative damage as

$$D(t, L) = 1 = \sum_{i=1}^{\nu \cdot t} \Delta D_i \approx \nu \cdot t \cdot \mathbb{E}[\Delta D_i|\gamma_c], \quad (12)$$

where  $\nu$  is the average number of stress cycles in a year, which is assumed to be  $10^5$  cycles/year.

The expected damage per fatigue cycle can be elaborated using the model in Eq. (10):

$$\mathbb{E}[\Delta D_i|\gamma_c] = \mathbb{E}\left[\frac{1}{N_F(\Delta S_e, \gamma_c)}\right] = \frac{1}{k \cdot \delta_1} \cdot \Delta S_e^m \cdot \gamma_c^{-\beta_2}, \quad (13)$$

where  $\Delta S_e$  is the equivalent stress range of the wave-induced stress process  $\Delta S(t)$ , which is defined as the constant stress that leads to the same accumulated damage as the time-dependent process.  $\Delta S_e$  is assumed to be Weibull distributed with parameters  $k_w$  and  $\lambda_w$ . Then  $\Delta S_e$  is given by

$$\Delta S_e = \mathbb{E}_{\Delta S}[\Delta S(t)^m]^{1/m} = k_w \cdot \Gamma\left(1 + \frac{m}{\lambda_w}\right)^{1/m}, \quad (14)$$

where  $\Gamma(\cdot)$  is the complete gamma function. This expression is substituted in Eq. (13) to compute the expected damage per cycle.

The equivalent stress range  $\Delta S_e$  is calibrated so that the uncorroded mooring line segment is associated with a target cumulative probability of fatigue failure of  $10^{-5}$  at the end of service life when no inspections nor repairs are conducted. Note that this target probability of failure is somewhat larger than the requirements in some offshore standards, such as DNVGL-OS-E301<sup>4</sup>, which is typically prescribed to be  $10^{-3}$ . The reason for this is that these standards do not consider the effect of pitting corrosion in the fatigue limit state. We assume that the mooring lines were provided at design with some additional safety to accommodate for the additional contribution of corrosion to fatigue failure. The mean value of  $k_w$  is calibrated to match the target probability

**Table 4.** Calibration of the expected shape parameter of the Weibull distributed fatigue stresses  $\mathbb{E}[k_w]$  as a function of the service life of the mooring life  $T_{SL}$  for a target probability of failure of  $10^{-5}$ .

$T_{SL}$ [years]	20	25	30	35	40
$\mathbb{E}[k_w]$ [N/mm <sup>2</sup> ]	5.1	4.7	4.4	4.2	4.0

of failure, where  $k_w$  is assumed to be Log-normal distributed with coefficient of variation (CoV) equal to 0.22, and  $\lambda_w$  is deterministic and equal to 0.8. Some values of the calibrated parameter are given in Table 4 for service lives  $T_{SL}$  between 20 and 40 years.

The probability of failure of a mooring line segment with a remaining service life of  $t$  years and subject to a corrosion level  $\gamma_c$  is denoted  $P_{f|\Gamma_c}$  and assessed using the a limit state function (LSF)  $g$

$$P_{f|\Gamma_c}(t) = \Pr[g(\mathbf{x}; t|\gamma_c) \leq 0], \quad (15)$$

where  $g \leq 0$  defines the failure domain and  $\mathbf{X}$  is a vector collecting the involved random variables, which have a joint probability distribution distribution  $f_{\mathbf{X}}(\mathbf{x}; t)$  defined via the BN model.

The limit state function  $g$  can then be written according to the Palmgren-Miner failure criterion<sup>22</sup>

$$g(\mathbf{x}; t|\gamma_c) = \Delta - D(\mathbf{x}; t|\gamma_c), \quad (16)$$

where  $D(\mathbf{x}; t|\gamma_c)$  is given by Eq. (12) and  $\Delta$  is a random variable representing the uncertainty associated with the fatigue failure criterion. JCSS<sup>23</sup> recommends to model  $\Delta$  by a Log-normal distribution with mean 1 and CoV 0.3.

The probability of failure of a mooring line segment is defined conditional on its corrosion level by Eq. (15). This equation can be evaluated with standard structural reliability methods, such as the first order reliability method (FORM). Note that the LSF depends on the fatigue damage accumulated during a period  $t$ . During this time, an equivalent fatigue stress is introduced to represent the effect of the wave-induced stress range distribution. However, an equivalent corrosion level is not available in the literature. Corrosion is a complex deterioration process that evolves with time. We assume as a simplification that the corrosion condition can be regarded as constant within a reference period of about a year.

## The Bayesian network

A BN is a directed acyclic graph consisting of nodes and arcs. The nodes represent the variables of interest, with

discretized sample space in our case, and the arcs between the nodes represent the dependencies. A BN is a convenient representation of the problem where explicit use of causal relations is incorporated via the arrangement of the network. Moreover, the BN model allows efficient inference of the conditional distributions when data become available at a subset of nodes. The BN is formally represented on the computer by a list of nodes and its neighbors along with conditional probability tables (CPTs) for each variable. The Bayes Net Toolbox<sup>24</sup> is used for computing the models in MATLAB<sup>®</sup>.

We propose a BN with 8 layers to represent the dependence structure of the decision problem. A summary of the layers is shown in Table 5 and a brief description is provided hereafter.

- Layer 1: at the highest layer of the network we have the hyperparameter  $\alpha_T$ , which is used to introduce statistical dependence among the temperature at the different water depths.
- Layer 2: this layer is constituted by the nodes of the influencing parameters of pitting corrosion, which in our model is only the temperature nodes  $T_s$ . Note that  $T_s$  refers to the yearly average temperature of the segments  $S_{i,j,s}$ . The temperature nodes are represented by a discrete distribution.
- Layer 3: here we have the maximum pit depth nodes  $d_{i,j,s}$ , which are specified conditional on the corresponding temperature  $T_s$ .
- Layer 4: this layer is constituted by the corrosion level nodes  $\gamma_{c,i,j,s}$ . Each of them is specified conditional on the corresponding maximum pit depth node  $d_{i,j,s}$ .
- Layer 5: In order to assess the integrity of a segment  $E_{S,i,j,s}$ , the accumulated probability of fatigue failure of the segment is computed conditional on its corrosion level  $\gamma_{c,i,j,s}$ .
- Layer 6: the integrity of a mooring line  $E_{L,i,j}$  is specified conditional on the integrity of its segments  $E_{S,i,j,s}$ , with  $s = 1, 2, \dots, p$ .
- Layer 7: a simplified ultimate limit state is introduced to specify the integrity of a cluster  $E_{C,j}$  conditional on the state of its lines  $E_{L,i,j}$ , with  $i = 1, 2, \dots, N_j$ .
- Layer 8: the integrity of the mooring system  $E_{sys}$  is calculated conditional on the state of the clusters  $E_{C,j}$ , with  $j = 1, 2, \dots, M$ .

The modeling of the dependence structure in the BN (Layers 1-3) and the implementation of the structural integrity model (Layers 4-8) are elaborated in more detail hereafter.

**Table 5.** Layers of the Bayesian network, with a description of the nodes.

Layer	Description	Node
Layer 1	Hyperparameter	$\alpha_T$
Layer 2	Temperature	$T_s$
Layer 3	Max pit depth	$d_{i,j,s}$
Layer 4	Corrosion level	$\gamma_{c,i,j,s}$
Layer 5	Segment integrity	$E_{S,i,j,s}$
Layer 6	Line integrity	$E_{L,i,j}$
Layer 7	Cluster integrity	$E_{C,j}$
Layer 8	System integrity	$E_{sys}$

### Statistical dependence model

The statistical dependence of the corrosion condition among line segments is captured in the BN in two ways, see Figure 4. First, the dependence of the corrosion condition among segments belonging to the same partition  $s$  of the mooring lines is modeled by conditioning the maximum pit depth nodes  $d_{i,j,s}$  on the corresponding temperature node  $T_s$ . Second, the dependence among the condition of segments from different partitions is modeled through the statistical dependence of the seawater temperature at different water depths. This correlation is introduced by conditioning the seawater temperature nodes on a hyperparameter  $\alpha_T$ . A Gaussian copula with given correlation coefficient is used to represent the joint distribution of the temperature nodes, according to the approach proposed by Luque and Straub<sup>25</sup>.

Other parameters of the employed deterioration model may be correlated among different chain segments. The consideration of additional parameter correlations would

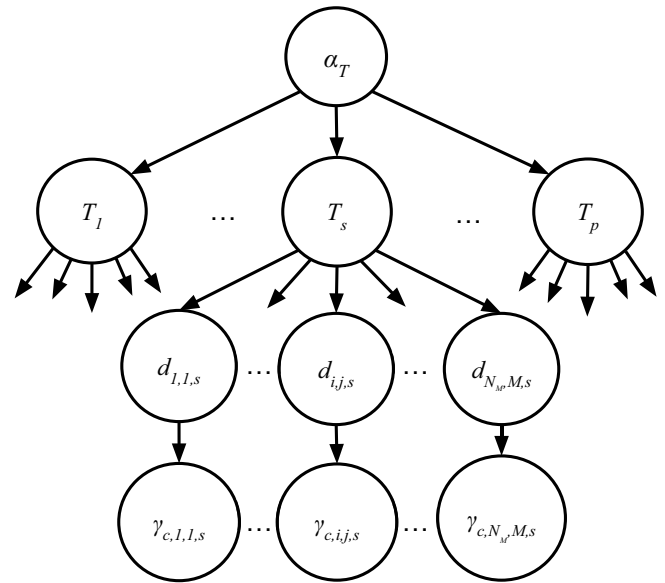


**Figure 4.** Hierarchical structure of the upper layers of the Bayesian network. The corrosion level nodes  $\gamma_{c,i,j,s}$  are specified conditional on the maximum expected pit depth nodes  $d_{i,j,s}$ , which in turn are specified conditional on the temperature node of the corresponding water depth  $T_s$ . The temperature nodes are correlated through the hyperparameter  $\alpha_T$ .

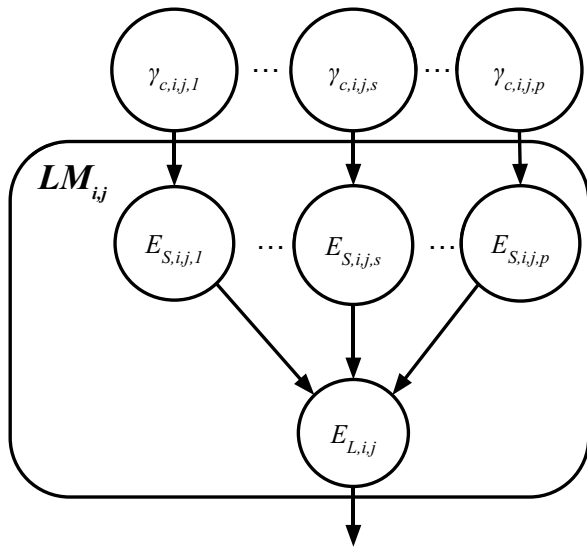


**Figure 5.** Module  $LM_{i,j}$  modeling the structural integrity a mooring line  $E_{L,i,j}$  as a serial system of the line segments  $E_{S,i,j,1}, \dots, E_{S,i,j,p}$ .

require to explicitly represent those parameters in the BN. This would largely increase the complexity of the BN. Since the aim of the decision framework is to rank the efficiency of inspecting chain segments, the authors have prioritized to limit the computational demand of the BN and not to include these additional correlations. However, this would not be justified if an accurate estimation of the reliability of the mooring system would be needed to e.g. include target reliability constraints.

### Mooring line integrity

The structural integrity of the  $p$  segments is denoted  $E_{S,i,j,1}, \dots, E_{S,i,j,p}$ , respectively. The fatigue integrity of a line  $L_{i,j}$ , denoted  $E_{L,i,j}$ , is defined conditional on the integrity of its segments, as illustrated in Figure 5. Note that the integrity of the segments is conditional on their corrosion level. Both the integrity of a segment and of the whole line have a binary representation (0: *Safe* or 1: *Fail*). Therefore, the CPT of  $E_{L,i,j}$  needs to be defined for  $2^p$  combinations of the segments states. The CPT mainly consists of zeros and ones, since the mooring line survives only when all its segments take the *Safe* state and fails in all other situations.

### Integrity of a cluster of mooring lines

The modeling of the integrity of a cluster of mooring lines  $E_{c,j}$  is shown in Figure 6.  $E_{c,j}$  has a binary representation (0: *Safe* or 1: *Fail*). It is assumed that the undamaged cluster is associated with an annual probability of failure of  $10^{-5}$ , as prescribed in DNVGL-OS-E301.<sup>4</sup> The probability of failure of a cluster conditional on the number of failed

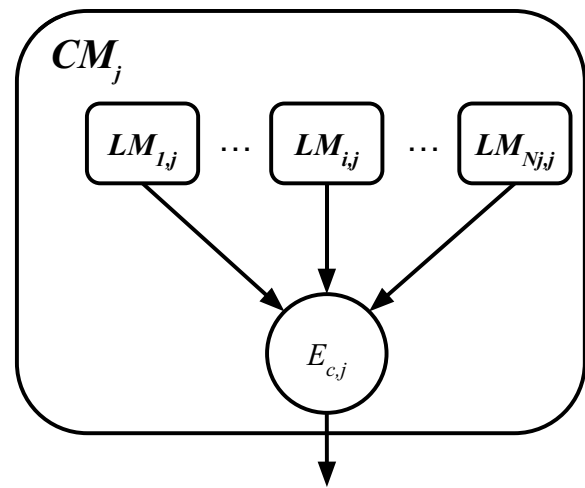


**Figure 6.** Module  $CM_{i,j}$  modeling the structural integrity of a cluster  $E_{c,j}$ , which constituted by  $N_j$  parallelly connected mooring lines.

lines  $\Pr(E_{c,j} = Fail | N_F = \ell)$  is computed assuming brittle failure due to ultimate load, i.e. a failed line does not contribute to load bearing. The probability of cluster failure conditional on the number of failed lines is then given by

$$\Pr(E_{c,j} = Fail | N_F = \ell) = \int_Q \Pr[E_{c,j} = Fail | q, (N_j - \ell)] f_Q(q) dq, \quad (17)$$

where  $f_Q$  is the probability density function of the annual extreme load  $Q$  and  $\Pr[E_{c,j} = Fail | q, (N_j - \ell)]$  is the probability of failure of the cluster conditional on the load and the number of survived lines, which is computed according to the solution by Daniels.<sup>26</sup>

It is assumed that the lines of a cluster have independent and identically distributed ultimate load capacity  $R_i$ , which is Log-normal distributed with CoV 0.15. The ratio between the mean capacity of the undamaged cluster, i.e.  $N_j \cdot \mu_{R_i}$ , and the mean annual maximum load  $\mu_Q$  is calibrated so that the cluster has the appropriate probability of failure in the undamaged state.  $Q$  is assumed to be Gumbel distributed with CoV 0.3. The conditional probability of failure of a cluster is plotted in Figure 7 for clusters containing different number of mooring lines  $N_j$ .

### Structural integrity of the mooring system

The structural integrity of the mooring system  $E_{sys}$  is represented in the BN by a node with two states: 0: *Safe* or 1: *Fail*. The integrity of the system depends on the integrity of the different clusters conforming it. This dependence is case dependent and it is influenced by the configuration of the anchoring system of the offshore floating unit. It is often the case that the failure of a cluster of mooring



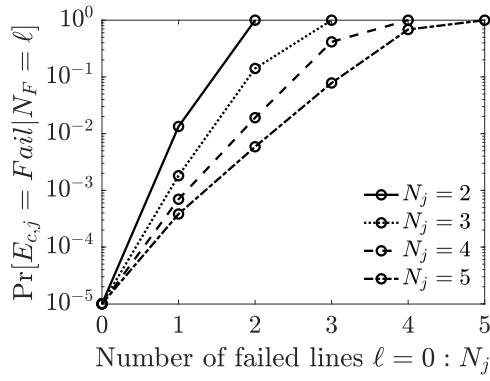


**Figure 7.** Conditional probability of failure of a cluster with  $N_j$  mooring lines for increasing number of failed lines  $\ell$ .

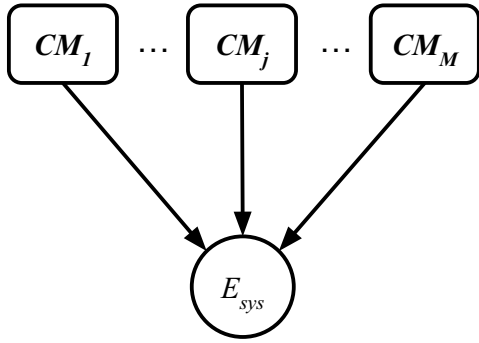


**Figure 8.** Structural integrity  $E_{sys}$  of the mooring line system constituted of  $M$  mooring clusters.

lines leads to loss of sufficient anchorage and consequently to disproportionate consequences, such as oil spill and associated loss of reputation. The BN model of the integrity of the mooring system is illustrated in Figure 8. Note that,  $E_{sys}$  is conditional on the integrity of the clusters  $E_{c,j}$ , with  $j = 1, \dots, M$ , which are defined by the module  $CM_j$  in Figure 6.

### Case study

The potential benefits of the presented framework are demonstrated alongside a case study on optimal inspection planning for the mooring system of an oil and gas platform in the North Sea. The case study contains several simplifications to keep the complexity in comprehensible limits.

The considered mooring system consists of four clusters, each of them with four mooring lines. The mooring system fails if any of the clusters fail. It is assumed that all the mooring lines have been placed at the same time, and no repairing or replacement have been conducted prior to the assessment. The platform is located in an area where the average water depth is ca. 100 m. The focus is on the submerged parts of the mooring lines, which are divided

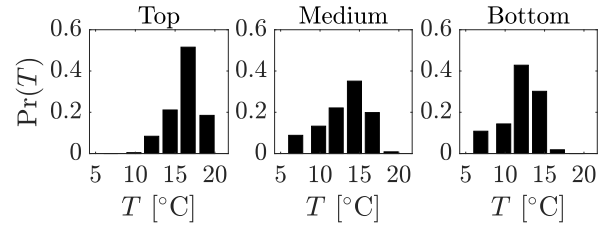


**Figure 9.** Probability mass function  $\Pr(T)$  of the average seawater temperature at top, medium and bottom locations.

in three segments; the top segment ranging in the water depth 0 - 20 m, the medium segment ranging in the water depth 20 - 50 m and the bottom segment ranging deeper than 50 m. In this case study, the VOI of inspecting the corrosion condition of the different segments is assessed. The simultaneous observation of several segments during one inspection campaign is not considered for simplicity.

The assumptions for distribution and correlation of water temperature are based on observations collected at the UK shelf.<sup>27</sup> The yearly average temperature in each depth segment is modeled with the probability mass functions in Figure 9, which has a discretization of intervals of ca. 3°C from the minimum to the maximum temperature, which are 5.5°C and 20.7°C, respectively. The temperature is averaged over observations at each interval, which corresponds to the values shown in Table 1. The linear correlation coefficient among the average temperature of the segments is found to be around 0.8.

The structure was designed with a service life of 30 years. Hence, the expected shape parameter of the fatigue stress range is taken as  $\mathbb{E}[k_w] = 4.4 \text{ N/mm}^2$ , according to Table 4. The current analysis considers potential inspections at year five and the projections of the structural integrity are assessed for an additional year, i.e. potential failure between years five and six. It is assumed that the corrosion condition can be considered constant during one year.

A series of actions or decision alternatives that the decision maker can choose from are to be specified to define the value function in Eqs. (1) and (2). It is noted that the VOI of an inspection scheme depends largely on the consideration of these actions. We provide a variety of decision alternatives in order to mimic the multiple options that would be explored in a more realistic sequential decision analysis, where not only repair options but also additional sequential inspection alternatives would be assessed. The representation of the latter would be by far too complex for this case study. Here, the decision maker can choose to not take any action ( $a = 0$ ), to repair the top, medium, or bottom segment of a given line (denoted  $a = 1$ ,  $a = 2$  and  $a = 3$ , respectively) or to repair the top, medium, or bottom segment of one line per cluster

( $a = 4$ ,  $a = 5$ ,  $a = 6$ ). Furthermore, the decision maker can replace a complete line in a cluster ( $a = 7$ ) or a complete line in each cluster ( $a = 8$ ). It is also possible to repair all the top, medium and bottom segments of a cluster ( $a = 9$ ,  $a = 10$ ,  $a = 11$ ) or of the entire system ( $a = 12$ ,  $a = 13$ ,  $a = 14$ ).

Assuming that inspection results  $\mathbf{y}_\kappa$  can be available, the PPV calculation requires the expected values for all possible observation outcomes. For the PV, the inspection just denotes the empty set. First, for the alternative of no repair or replacement ( $a = 0$ ), the expected value is then defined as

$$\mathbb{E}[v(\mathbf{x}, 0)|\mathbf{y}_\kappa] = -c_l \max_{i,j} \{ \Pr(E_{L_{i,j}} = 1 | \mathbf{y}_\kappa) \} - c_s \Pr(E_{sys} = 1 | \mathbf{y}_\kappa), \quad (18)$$

where  $c_l$  is the cost of failure of a mooring line and  $c_s$  is the cost of system failure. Here,  $c_l$  is taken as € 20 mln and it is mainly associated with the cost of replacing the failed line, including the production loss from the detection of the failure until the line is replaced. The consequences of system failure is taken as  $c_s = € 180$  mln.

For the other alternatives  $a > 0$ , we let  $\gamma_c(\mathbf{x}_a)$  denote the corrosion level of the segments that have been repaired or replaced and consequently returned to the uncorroded state, i.e.  $\gamma_c(\mathbf{x}_a) = 1$ . The expected values are then

$$\mathbb{E}[v(\mathbf{x}, a)|\mathbf{y}_\kappa] = -c_l \max_{h,l} \{ \Pr(E_{L_{h,l}} = 1 | \gamma_c(\mathbf{x}_a) = 1, \mathbf{y}_\kappa) \} - c_s \Pr(E_{sys} = 1 | \gamma_c(\mathbf{x}_a) = 1, \mathbf{y}_\kappa) - c_a n_a, \quad (19)$$

where  $c_a = \{c_r, c_{rl}\}$  is the cost of repairing ( $c_r = € 0.7$  mln) or replacing ( $c_{rl} = € 0.9$  mln) a segment depending on the decision taken, and  $n_a$  is the number of segments that are repaired or replaced; The costs  $c_a$  are assumed to be the same for all segments.

Given the structure of the value function, and that we deal with discretizations of the continuous distributions, it is possible to explicitly compute the PV and PPV. VOI analysis, as formally introduced above, is used in the following to select which segments to inspect.

## Results

VOI analysis is first performed with the assumed standard deviation of the pitting corrosion model uncertainty set to  $\sigma_{\delta_2} = 0.5$ . Afterwards, the effect of increasing or reducing the model accuracy is investigated.

The effect of observing the corrosion condition of different segments on the assessment of the probability of failure of a line is illustrated in Figure 10. The effect of observing

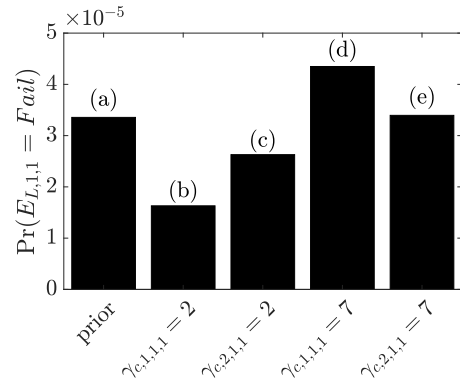


**Figure 10.** Effect of belief propagation on the probability of failure of a line  $\Pr(E_{L_{1,1}} = Fail)$ . Evidence of low corrosion in the top segments of the assessed line and a nearby one is shown in (b) and (c), respectively. (d) and (e) present the effect of observing high corrosion in the same segments.

the corrosion condition of a segment of the line of interest can be seen in cases (b) and (d). Observing a low corrosion level ( $\gamma_c = 2$ ) decreases the probability of failure by approximately half with respect to the prior case, and an observation of a high corrosion level ( $\gamma_c = 7$ ) increases it by 30%. Inference from observations of a segment of a different line are shown in (c) and (e) and show as well a considerable effect, although weaker than for (b) and (d).

The computation of the VOI is conducted for a given line of the system, where single observations of the corrosion level are possible. Note that these results are valid for any line of the system due its symmetry in terms of number of segments and of number of lines in a cluster. Table 6 summarizes the results of the VOI analysis for the three segments (top, medium and bottom). The obtained VOI can be used to assess the most valuable location for inspection. The results show that observing the corrosion level of the top segments is the most valuable inspection.

The sensitivity of the results with respect to the modeling error as parametrized by the standard deviation  $\sigma_{\delta_2}$  is studied. Table 7 shows a decrease of the VOI as the standard deviation increases. On the one hand, a large uncertainty in the estimation of the maximum pit depth results in a less informative prior assessment. This suggests that newly obtained information has the potential to drastically change the expectation of the system condition. On the other hand, a large model uncertainty also yields a broad

**Table 6.** Results of VOI analysis for observations of the corrosion level of the top, medium and bottom segment of a given line, when the decision alternatives are the ones described in the case study section.

	Top	Medium	Bottom
VOI	€285	€278	€283

**Table 7.** Results of VOI analysis for the observation of the corrosion level of the top, medium and bottom segment of a given line for different values of the standard deviation of the multiplicative model error  $\sigma_{\delta_2}$ .

	Top	Medium	Bottom
VOI at $\sigma_{\delta_2} = 0.1$	€294	€298	€304
VOI at $\sigma_{\delta_2} = 0.3$	€292	€289	€295
VOI at $\sigma_{\delta_2} = 0.7$	€272	€264	€269
VOI at $\sigma_{\delta_2} = 0.9$	€260	€250	€254

**Table 8.** Results of VOI analysis for observations of the corrosion level of the top, medium and bottom segment of a given line after 10 years of service life of the system.

	Top	Medium	Bottom
VOI	€6225	€6223	€6239

likelihood function of the inspection outcomes, which reduces the efficiency of the inspections. We argue that due the large costs associated with the mitigation actions and the consequences of failure, the latter has a larger impact on the results. The fact that new observations become more valuable when the model accuracy increases emphasizes the importance of uncertainty quantification and the development of an accurate model for pitting corrosion degradation. It is observed that the most valuable inspection switches from being the bottom segment inspection to be the top segment inspection for a value of  $\sigma_{\delta_2}$  somewhere in between 0.3 and 0.5.

Finally, VOI is studied for a situation similar to the one of Table 6, where the only difference is that now the study is done after ten years of service life of the system. The larger VOI in Table 8 shows how gathering information on a more deteriorated system will be of greater value for the decision maker. This is due to the larger variation that the probability of failure of a line presents depending on the corrosion condition and due to the overall larger probability of system failure.

The computational complexity of the framework developed, is mostly associated with the evaluation of the VOI, assuming a BN is already set with all the CPT computed. For the preposterior value (PPV), a sum must be computed over the possible outcomes of the observation ( $y_k$ ), and for each outcome, the CPT are updated to get the conditional expressions. For each outcome, this takes only about 1 second, and overall the BN fitting and VOI calculation only take about 3 minutes on a commercial laptop with a 3.1 GHz Dual-Core Intel Core i7 processor. A benefit of BN models is that they represent the important variables in a compact manner and large size computer intensive evaluations are often avoided.

## Discussion

The proposed framework aims at supporting inspection planning decisions for mooring systems based on VOI analysis. Relevant features that affect the decisions at hand and their interactions are explicitly represented in a BN model. The framework is ultimately a simplification of a highly complex decision problem. The actual sequential decision problem is simplified by neglecting the effect of future inspections in the planning of inspections at a given year. Furthermore, the assessment of the structural reliability is conducted with projections of an additional year from the decision point in time. This leads to low estimates of the probability of failure, which in turn leads to low estimates of the VOI. As a consequence, the results of the analysis cannot be used to determine whether inspections should be conducted, but only to rank which inspections should be conducted first. It is nonetheless common practice that the decision maker first chooses if it is needed to conduct inspections, and then decides what to inspect. The proposed framework can be used in the second step to guide that type of decision.

Currently available models for pitting corrosion are associated with large uncertainties. Despite these uncertainties, integrity management decisions need to be made. This stresses the importance of uncertainty quantification and of integrating these uncertainties into a formal framework in order to support decisions according to the best available knowledge. More accurate modeling of the deterioration processes could be added when available to improve the quality of the outcomes. Results from the case study show the value of improving the model accuracy, see Table 7.

A simplified model is used to assess the fatigue integrity of a mooring segment conditional on its corrosion condition. Since the corrosion condition evolves with time, the unconditional probability of failure should be dynamically assessed. The obtained estimation of the probability of failure at a given year  $t$  is thus a conservative approximation in which the corrosion at that year is used to represent the condition at all the previous years. This is justified at the early stages of the deterioration due to the power-law growth of corrosion, in which pits rapidly reach significant depths followed by a steadier growth. If the lifetime cumulative probability of failure of a mooring line segment was to be more accurately computed, the unconditional limit state function  $g(\mathbf{x}; t = T_{SL}) \leq 0$  should be considered instead of Eq. (16), where  $g(\mathbf{x}; t)$  is defined as

$$g(\mathbf{x}; t) = \Delta - \sum_{\tau=1}^t \sum_{\Gamma_c} D(\mathbf{x}; \tau | \gamma_c) \Pr(\gamma_c; \tau). \quad (20)$$

A dynamic BN should be developed to evaluate this equation. This BN would drastically increase the computational demand as compared to the one proposed in this article. Nonetheless, it is unclear whether this would lead to significantly better decisions.

## Conclusions

A method based on value of information analysis is presented in this paper with the aim of supporting efficient planning of in-situ inspections of the corrosion condition of structural elements of a mooring systems. We focus on the particular case of mooring systems constituted by steel chain mooring lines. Chain links in marine conditions are subject to pitting corrosion, which leads to an increased probability of fatigue failure of the chain links under cyclic loading. An ultimate load limit state is used in order to assess the integrity of the deteriorating system, which is subject to a combination of pitting corrosion and fatigue. A state-of-the-art model is used to model the growth of corrosion pits in time. The model assumes that pit growth is mainly caused by the action of sulfate reducing bacteria under anaerobic conditions, which is driven by the average seawater temperature at a given location.

The mooring system is regarded as hierarchically structured with four levels: (i) the mooring system, (ii) the cluster of mooring lines, (iii) the mooring line and (iv) the line segment, which is constituted by a number of chain links. We propose a Bayesian network to model statistical dependence of the corrosion among line segments and to estimate the structural integrity of the mooring system. The network allows for efficient updating of the corrosion condition of the mooring segments and reassessment of the integrity of the system when new observations become available. This allows to efficiently conduct value of information analysis, which is used to rank inspection alternatives. The application of the framework is illustrated with a case study. Results emphasize the importance of the accuracy of the corrosion model to increase the value of the inspections.

## Acknowledgements

The authors would like to acknowledge the members of the KPN Lifemoor project for the discussions and useful insight.

## References

- Fontaine E, Kilner A, Carra C et al. Industry survey of past failures, pre-emptive replacements and reported degradations for mooring systems of floating production units. In *Offshore Technology Conference*. Offshore Technology Conference.
- API. Design and analysis of stationkeeping systems for floating structures, third edition. In *API RP 2SK*. Washington, D.C, USA: API Publishing Services, 2015.
- ISO. ISO 19901-7:2013: Petroleum and natural gas industries - specific requirements for offshore structures — part 7: Stationkeeping systems for floating offshore structures and mobile offshore units. techreport, International Organization for Standardization, Geneva, Switzerland, 2013.
- DNV-GL. Position mooring. In *DNVGL-OS-E301*. DNV-GL, 2015.
- Pérez-Mora R, Palin-Luc T, Bathias C et al. Very high cycle fatigue of a high strength steel under sea water corrosion: A strong corrosion and mechanical damage coupling. *International Journal of Fatigue* 2015; 74: 156 – 165. DOI:<https://doi.org/10.1016/j.ijfatigue.2015.01.004>.
- Arredondo A, Fernández J, Silveira E et al. Corrosion fatigue behavior of mooring chain steel in seawater. In *ASME 2016 35th International Conference on Ocean, Offshore and Arctic Engineering*. American Society of Mechanical Engineers Digital Collection.
- Morgantini M, MacKenzie D, Gorash Y et al. The effect of corrosive environment on fatigue life and on mean stress sensitivity factor. In *MATEC Web of Conferences*, volume 165. EDP Sciences, p. 03001.
- Kondo Y. Prediction of fatigue crack initiation life based on pit growth. *Corrosion* 1989; 45(1): 7–11.
- Cerit M, Genel K and Eksi S. Numerical investigation on stress concentration of corrosion pit. *Engineering Failure Analysis* 2009; 16(7): 2467–2472.
- Gabrielsen Ø, Larsen K and Reinholdtsen SA. Fatigue testing of used mooring chain. In *ASME 2017 36th International Conference on Ocean, Offshore and Arctic Engineering*. American Society of Mechanical Engineers Digital Collection.
- Lindley T, McIntyre P and Trant P. Fatigue-crack initiation at corrosion pits. *Metals technology* 1982; 9(1): 135–142.
- Gordon RB, Brown MG, Allen EM et al. Mooring integrity management: a state-of-the-art review. In *Offshore Technology Conference*. Offshore Technology Conference.
- Straub D and Der Kiureghian A. Reliability acceptance criteria for deteriorating elements of structural systems. *Journal of Structural Engineering* 2011; 137(12): 1573–1582.
- Luque J, Hamann R and Straub D. Spatial probabilistic modeling of corrosion in ship structures. *ASCE-ASME Journal of Risk and Uncertainty in Engineering Systems, Part B: Mechanical Engineering* 2017; 3(3): 031001.
- Raiffa H and Schlaifer R. *Applied statistical decision theory*. Cambridge University Press, 1961.

16. Eidsvik J, Mukerji T and Bhattacharjya D. *Value of information in the earth sciences: Integrating spatial modeling and decision analysis*. Cambridge University Press, 2015.
17. Chan TU, Hart BT, Kennard MJ et al. Bayesian network models for environmental flow decision making in the daly river, northern territory, australia. *River Research and Applications* 2012; 28(3): 283–301.
18. Martinelli G, Eidsvik J, Sinding-Larsen R et al. Building bayesian networks from basin-modelling scenarios for improved geological decision making. *Petroleum Geoscience* 2013; 19(3): 289–304.
19. Arzaghi E, Abbassi R, Garaniya V et al. Developing a dynamic model for pitting and corrosion-fatigue damage of subsea pipelines. *Ocean Engineering* 2018; 150: 391–396.
20. Li X, Zhu H, Chen G et al. Optimal maintenance strategy for corroded subsea pipelines. *Journal of Loss Prevention in the Process Industries* 2017; 49: 145–154.
21. Melchers RE. Pitting corrosion of mild steel in marine immersion environment—Part 1: Maximum pit depth. *Corrosion* 2004; 60(9): 824–836.
22. Miner MA. Cumulative Damage in Fatigue. *Journal of Applied Mechanics* 1945; 12(3): 159–164.
23. JCSS. Probabilistic Model Code. Part 3: Resistance Models. Standard, Joint Committee of Structural Safety, 2001.
24. Murphy K et al. The bayes net toolbox for matlab. *Computing science and statistics* 2001; 33(2): 1024–1034.
25. Luque J and Straub D. Reliability analysis and updating of deteriorating systems with dynamicBayesian networks. *Structural Safety* 2016; 62: 34–46.
26. Daniels HE. The statistical theory of the strength of bundles of threads. i. *Proceedings of the Royal Society of London Series A Mathematical and Physical Sciences* 1945; 183(995): 405–435.
27. Morris et al. ScanFish – North and Celtic Seas, 2016. DOI: <https://doi.org/10.14466/CefasDataHub.20>.